ICAS 2021 SHANG HAI
International Council of the Aeronautical Sciences
32nd Congress of the International Council of the Aeronautical Sciences
September 6-10, 2021
Pudong Shangri-La, Shanghai, China

Circulation Control Aircraft: Recent Developments of the Channel-Wing Design

AHM. Faisal[1,2,*], AR. Abu Talib[1], AS. M. Rafie[1], & H. Djojodihardjo[3]

[1]Department of Aerospace Engineering, UPM, Serdang, Malaysia
[2]Aerospace Malaysia Research Centre (AMRC), UPM, Serdang, Malaysia
[3]The Institute for the Advancement of Aerospace Science and Technology, Jakarta, Indonesia

*mohd_faisal@upm.edu.my

Abstract

Recent development on the new generation of STOL/VTOL aircraft utilizing the active circulation flow control channel-wing design is presented. By redesign the wing into a half-circular shape and repositioning the propeller-blade at the trailing-edge, one could arrive in obtaining a suction effect that could enhance the generation of lift. The suction effect from the high speed rotating propeller mounted at the wing trailing-edge generates a high velocity slipstream, inducing the flow adjacent to the upper surface, reducing the pressure than the lower surface, generating lift. The characteristic of lift as a by product of its own thrust is something needs further attention. The amount of lift generated is quite impressive, increases with the amount of thrust produces. Results have shown that the amount of lift that could possibly be extracted reaching over one-third of its thrust. However, although gaining some lift, there will be some losses in the thrust; due to the viscous effect on the adjacent layer of fluid-wall.

Keyword*:* Channel-wing, aerodynamic force, lift-thrust, circulation control

1. Introduction

Over the years, air transportation has increasingly become an important driver in the movement of resources and wealth [1]. Despite having received such high demand, according to data from both the United States [2] and the European Union [3] airlines experience glitch, i.e. flight delays; with the majority of short-haul flights experiencing delays of up to 20%. For example, in the United States [4]–[6], airline flight delays have a staggering direct operating cost of approximately $8 billion USD per year. This must be addressed because it will result in additional delay compensation costs, especially for those who took the connecting flight.

Many brilliant ideas and solutions to this problem have been proposed. Some are proposing models to aid in simulating the problem of airline flight delay management, with the goal of optimising runway capacity by focusing on taxiway capacity and runway separation time [7], [8]. In addition, some research has been conducted to investigate the effect of aircraft wake vortex during arrival and departure in order to achieve efficient runway usage at any given time [9]–[13]. Aside from that, the incorporation of new elements in future aircraft design [14]–[18] is being researched in order to improve the aircraft's performance and make it more efficient and effective.

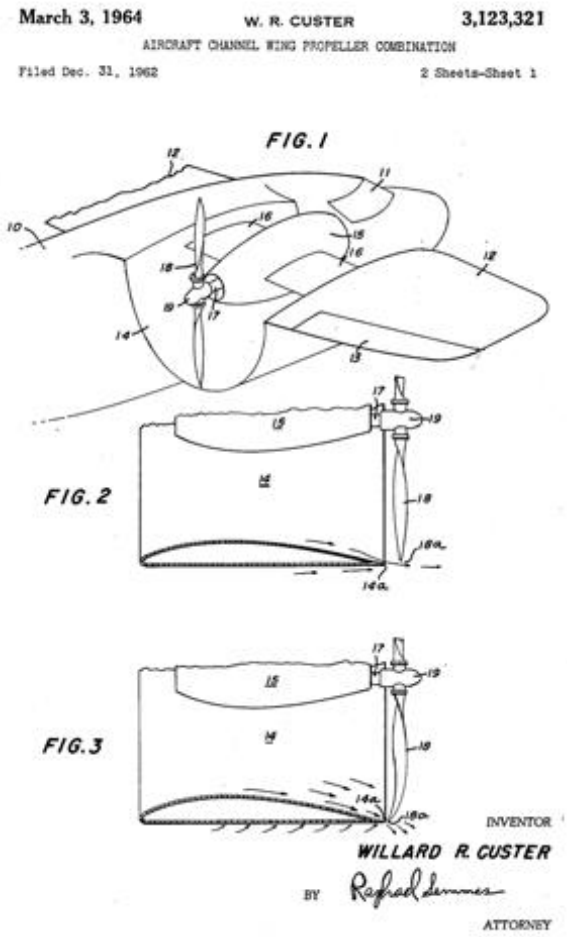

Figure 1 – From Willard Custer's patent: US3123321 A, published on 3rd March 1964 [19].

Modifying the conventional wing is critical for future aircraft; it opens up additional choices for addressing current challenges, such as short-haul flight issues. Incorporating active flow control technology to increase the aerodynamic efficiency of the wing is one of the finest solutions to examine [19–22]. This channel-wing aircraft utilized airflow entrainment to boost lift generation. As shown in Figure 1, one of the earliest examples is the patent filled in 1952 by Willard Custer, known as Custer Channel-wing Aircraft.

Unlike traditional fixed-wing aircraft, which rely on the aircraft's speed to generate lift, the channel-wing relied on the velocity of the airflow flowing over the wing. The pusher-type rotating propeller mounted at the trailing-edge of the wing entrained a high-velocity of airflow. This will induced a low pressure region on the wing-upper-surface. A net pressure difference between the lower and upper part of the wing will be created, hence, some amount of lift will be generated.

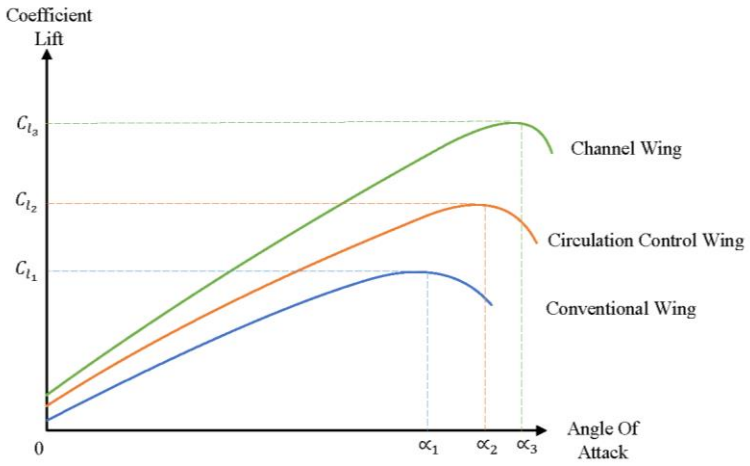

Figure 2 – Predictions on the aerodynamic lift performance of channel-wing as compared to circulation control wing and conventional wing.

An experimental study was previously conducted to evaluate the effect of wing sizing on the aerodynamic lift and propulsive thrust performances of channel-wing aircraft at rest [20]. The wing has been shown to be capable of extracting approximately 30% of the lift from the thrust. According to a study conducted at Georgia Tech Research Institute [21], the channel wing can produce nearly double the lift of a conventional aircraft equipped with a slotted flap. Developments and patents utilizing the active circulation control design have been presented through several research programs [22].

The channel-wing has the ability to produce lift even at zero forward velocity (stand-still). Also, able to work in a much broader range of the angle of attack before stall (as illustrated in Figure 2). Furthermore, under certain conditions it could also perform vertical take-off [21], [23], [24]. This paper will examine the aerodynamic performance of channel-wing aircraft at various flight speeds and angles of attack. The goal is to improve understanding (take-off ability) of channel-wing lift performance characteristics for future short-haul flight applications.

2. Methodology

2.1. Test bench setup

The channel-wing test bench setup consists of a channel-wing and a set of propeller-motor setup. The assembly and mounting positions of the main components of the channel-wing test bench setup are illustrates in Figure 3.

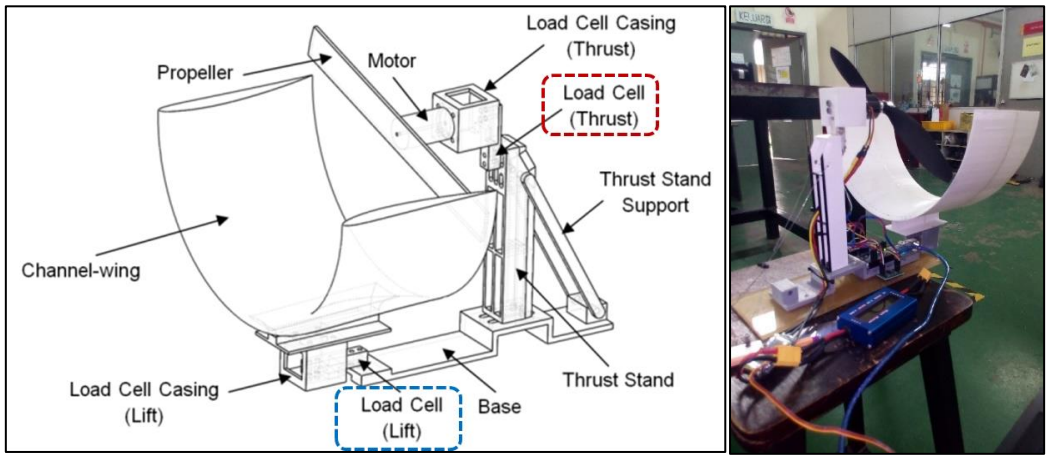

Figure 3 – Channel-wing test bench setup (left); Actual assembly of the channel-wing test bench setup (right).

The channel-wing profile is based on the NACA4412 airfoil [25]. For the wing chord length, it is measured as the ratio of the wing chord length (C_{wing}) to the propeller diameter (D_{prop}); measuring at 20%, 35%, and 55%, for the small, medium and large wing size, respectively.

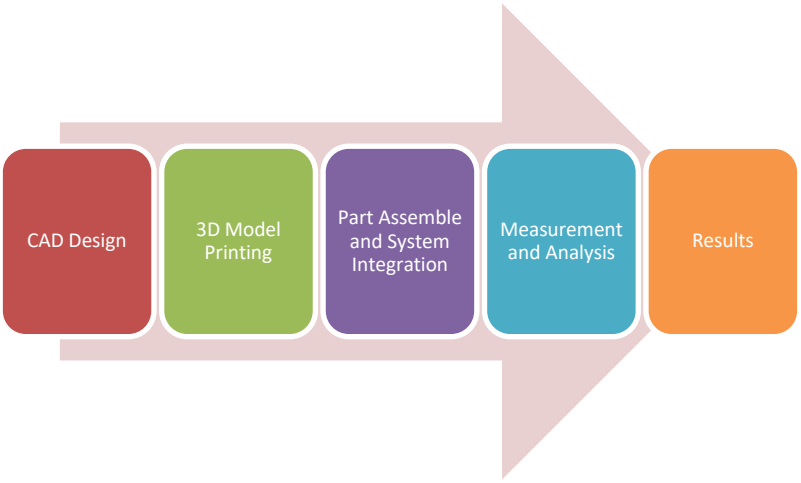

Figure 4 – The workflow of the experimental test setup for the channel-wing analysis.

The test model is created with CAD software and consists of numerous sections, all of which are constructed of Polylactic acid or polylactide (PLA) material and printed with a FDM 3D printer. For such a complicated design, the fabrication method is simple, rapid, and cost effective. The workflow of the experimental test setup (Figure 4) is similar to the one described previously; that is, a scaled-down model of the actual aircraft is utilised, with the propulsion unit placed to the rear side of the wing (similarly as illustrated in Figure 5).

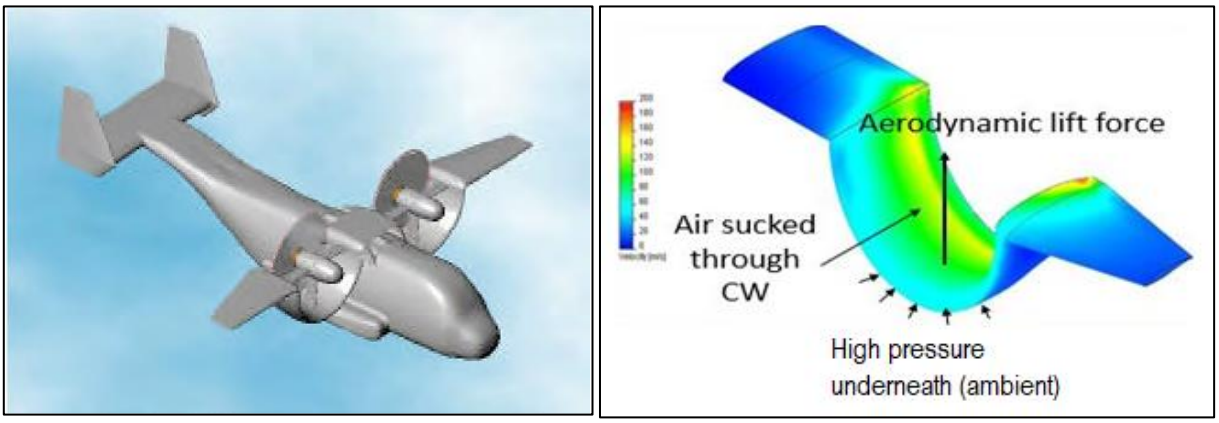

Figure 5 – Conceptual Pneumatic Channel-wing STOL aircraft [26] (left); Velocity field on the wing surface (right), adapted from Ref. [27].

For the thrust force generations, a 2-bladed propeller with a diameter of 250 mm (4.5 pitch) is used. It is aligned perpendicular to the trailing-edge section of the channel-wing. The clearance between the propeller-tip and the channel-wing surface is 1 to 2 mm.

The electrical components of the propeller-motor setup consist of $820\ kv$ motor, $30\ Amp$ ESC, DC watt meter, and Li-Po battery ($14.8V$). The schematic of the experimental setup is shown in Figure 6.

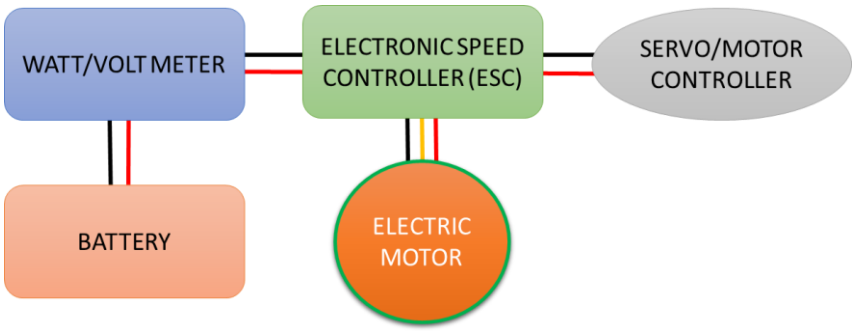

(a)

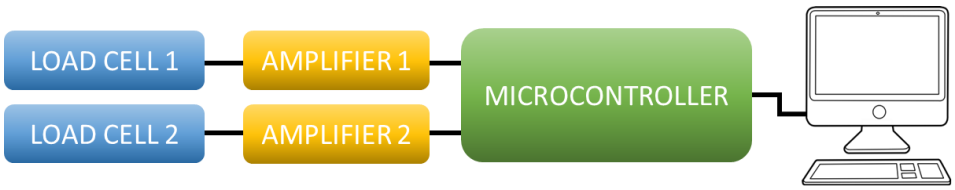

(b)

Figure 6 – (a) The schematic of the propeller-motor setup; (b) The schematic for the force/load measurement (lift and thrust).

2.2. Measurement process

Two load-cells are used for the force sensors measurement setup. Both are connected to the microcontroller that link to a compute. One measuring the lift force for the channel-wing and the other measure thrust force generate by the high-speed rotating propeller. The mounting position of the load cells:

1) Thrust force – it is mounted vertically, positioned in between load cell casing (thrust) and thrust stand support.
2) Lift force – it is mounted horizontally underneath channel-wing, connected to load cell casing (lift).

A microcontroller capable of processing data at the rate of 1000/s is used. It received input from load cells and transmits output data to the computer via micro USB cable.

2.3. Calibration & Error Analysis

Calibration for each of the load cell is done prior to each of the test with a set of dead weight (calibration up to 600 grams or ~6 N, with 50 grams increments). The indicated error for each of the load cell is measured ±0.5 grams. The measured data from the microcontroller is displayed and stored on the computer (data logger), and each data point (power, lift, thrust) is taken by taking the average of 50 readings. Table 1 provide a sample of data (i.e. power) for the uncertainty analysis of the experiment.

Table 1: Data for the uncertainty analyses

	Average Power (W)	Standard deviation	Error (%)
Small Channel-wing	5.33	0.12	2.34
	9.90	0.22	2.18
	15.00	0.22	1.44

	20.33	0.63	3.12
	25.03	0.31	1.23
	29.80	0.50	1.67
	34.93	0.83	2.39
	39.97	1.27	3.18
	45.27	0.41	0.91
Medium Channel-wing	5.33	0.05	0.88
	9.93	0.21	2.07
	14.97	0.39	2.58
	20.03	0.25	1.25
	25.03	0.17	0.68
	29.70	0.50	1.67
	34.97	0.33	0.94
	40.17	0.26	0.65
	45.10	0.08	0.18
Large Channel-wing	5.33	0.34	6.37
	9.90	0.29	2.97
	14.90	0.36	2.39
	20.20	0.65	3.23
	25.00	0.37	1.50
	30.00	0.24	0.82
	34.93	0.12	0.36
	40.20	0.33	0.81
	45.23	0.17	0.38
Without Channel-wing	5.30	0.08	1.54
	9.13	0.29	3.14
	14.97	0.17	1.14
	20.20	0.41	2.02
	24.90	0.75	3.01
	29.90	0.65	2.18
	35.37	0.54	1.54
	40.37	0.54	1.35
	45.30	0.79	1.74
Average Error (%)			**1.83**

Both of the measured thrust and lift forces as well as the indicated power supplied to the motor are recorded during the measurement process. The test is carried out in a control environment; the ambient temperature at 20° Celsius, air density of 1.225 kg/m^3 and humidity of 50%. Noted that average error (for all measured data) is below 5%, thus, the data taken are consider precise and accurate.

3. Results & Discussions

The test employs three distinct wing sizes: small, medium, and large. All tests are performed at zero forward speed and zero angle of attack. The amount of thrust force is shown to decrease when the channel-wing is fitted (as illustrated in Figure 7). The average reduction in thrust force when compared to the isolated propeller (or without channel-wing) is 11%, 13%, and 15% for small, medium, and large wing sizes, respectively.

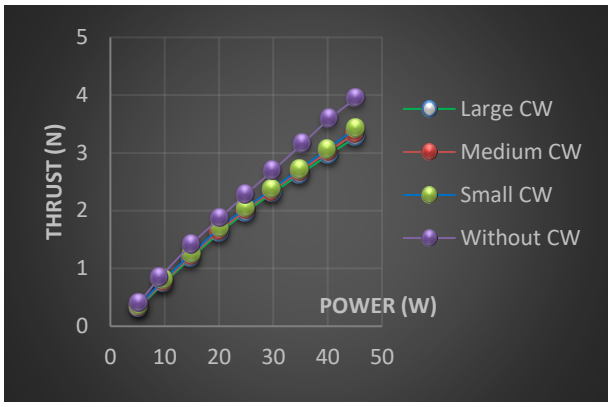

Figure 7 – Thrust force with and without channel-wing installed.

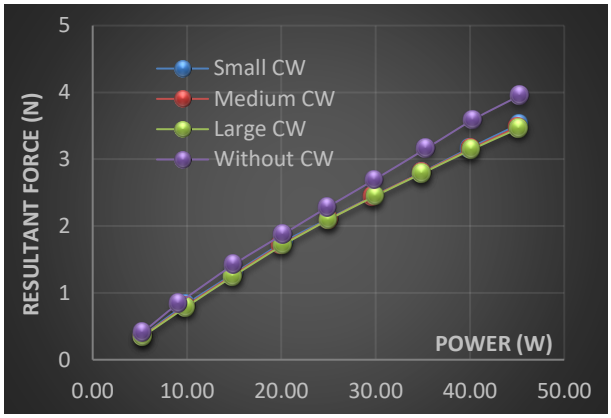

Figure 8 – Resultant force with and without channel-wing installed.

As shown in Figure 8, for the resultant force (i.e. lift and thrust components), with a channel-wing fitted, the resultant forces are dropped by 9%, 10%, and 11% for small, medium, and large wing sizes, respectively. The amount of thrust and the resulting force reductions are proportional to the length of the wing chord. With a greater wing chord, the air travels considerably further and picks up extra viscous forces, reducing the momentum of the airflow and hence the generated forces. The smaller wing (with shorter wing chord length) may have a little lower impact than the large one.

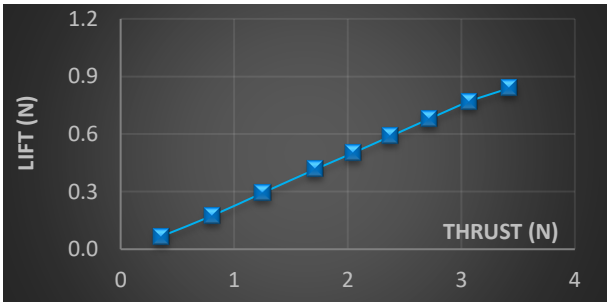

(a) For $\frac{C_{wing}}{D_{prop}} = 20\%$, small wing

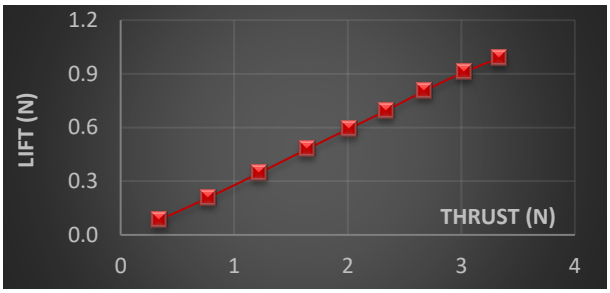

(b) For $\frac{C_{wing}}{D_{prop}} = 35\%$, medium wing

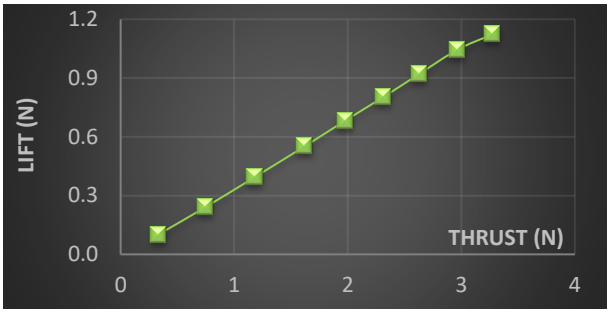

(c) For $\frac{C_{wing}}{D_{prop}} = 55\%$, large wing

Figure 9 – Changes in the lift force when the thrust force is increased

Figure 9 depicts the changes in lift as the thrust is increased. Increasing thrust has a favourable effect on lift generation. When comparing these three channel-wing sizes, the greater the wing chord length, the better the lift performance. This linear growth, on the other hand, will eventually plateau after reaching certain limits (i.e., when the value of thrust force exceeds 3.0 N).

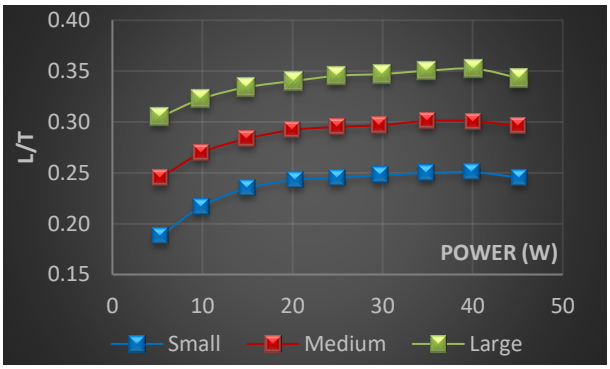

Figure 10 – The ratio between lift and thrust (L/T) for three different wing sizes ($\frac{C_{wing}}{D_{prop}}$).

The plotted lines for the lift to thrust ratio (L/T) versus power, as shown in Figure 10, can be classified into three stages: steep increase in the beginning, progressively flattens, and diminishes towards the end. The correlations and trends of change for all channel-wing sizes are proven to be consistent. The peak value of L/T increases from 25% to 30% and up to 35% for small, medium, and large wing sizes, respectively.

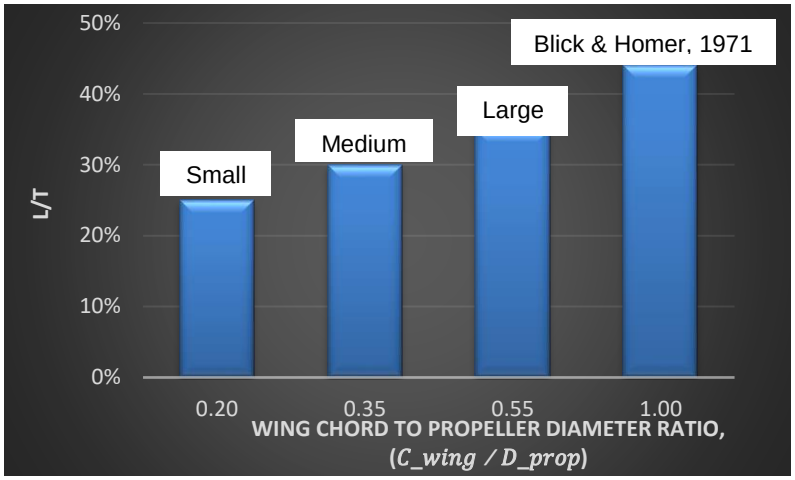

Figure 11 – Comparison of L/T for all three wings with the data presented by Ref. [25].

As shown in Figure 11, the L/T increase with the wing size. Large wing produce the highest L/T, compared to the medium and small wings. Thus, this shows that if one would like to obtain higher L/T (or to extract more lift force), the wing area should be relatively bigger. This finding is in agreement with the results obtained by Blick & Homer [25], the percentage of L/T could reach more than 40% for $\left(C_{wing}/D_{prop}\right)\sim 1$. In Ref. [25], the motor (which drives the propeller) is placed on the inside of the channel-wing, however, for the present setup, the motor is positioned on the outside. With this setup, it undisturbed the oncoming and entrainment of airflow on the inside of the channel-wing.

4. Conclusions

The aerodynamic lift force and propulsive thrust of the channel-wing design are evaluated at zero forward speed and zero angle of attack. The correlations/relationships between channel-wing lift and thrust, as well as the performance parameters derived from aerodynamic lift and propulsive thrust forces, are shown for three different sizes of wing chord length. Throughout the test, the input power supplied by the battery is increased in 5 watt increments from 5 to 45 watts. The motor is unable to run smoothly at less than 5 watts, and at more than 40 watts, the lift-thrust ratio is shown to decrease.

The high-velocity slipstream is created by a high-speed rotating propeller. A pressure difference between the upper and lower surfaces is created by the high velocity airflow adjacent to the upper surface, resulting in suction effects and lift. It demonstrates that a longer wing chord can extract significantly more lift. The amount of lift that could be extracted is over one-third of the thrust. Despite achieving some lift, there will be some thrust losses due to viscous effects on the adjacent layer of fluid-wall. Because the air encounters resistance as it flows and makes contact with the wing surface. For small wings, the losses are minimal, but for larger wings, the losses are much larger.

With more lift than conventional wing, the plane could take-off at a much slower speed and for a much shorter distance. Having extra lift means being able to carry more payloads. The aircraft will also save some fuel and maybe extend engine life (moving components are working at low revolutions/flight cycle) due to the shorter duration of high engine speed/blast at take-off. On a bigger picture, this study could provide an insight to overcome runway design constraints (conventional aircraft). The proposed channel-wing design could improve the aircraft's overall performance by allowing for engine capacity reductions, reduced fuel consumption and the amount of fuel carried, increased low-speed stability, lighter construction, and optimization of other subsystems.

Acknowledgement

The authors would like to the Universiti Putra Malaysia for providing the financial support through the Geran Putra IPM, Grant Agreements GP-IPM/2017/9537900.

Reference

[1] D. Y. Suh and M. S. Ryerson, “Forecast to grow: Aviation demand forecasting in an era of demand uncertainty and optimism bias,” *Transportation Research Part E: Logistics and Transportation Review*, vol. 128, 2019, doi: 10.1016/j.tre.2019.06.016.

[2] “US BUREAU OF TRANSPORTATION STATISTICS,” *United States Department of Transportation*. https://www.transtats.bts.gov/HomeDrillChart.asp (accessed Nov. 02, 2020).

[3] “EU Control.” https://www.eurocontrol.int/sites/default/files/2019-08/flad-june-2019.pdf (accessed Nov. 02, 2020).

[4] P. Belobaba, A. Odoni, and C. Barnhart, *The Global Airline Industry*. 2009. doi: 10.1002/9780470744734.

[5] E. B. Peterson, K. Neels, N. Barczi, and T. Graham, “The economic cost of airline flight delay,” *Journal of Transport Economics and Policy*, vol. 47, no. 1, 2013.

[6] J. F. O’Connell, “The global airline industry,” in *The Routledge Companion to Air Transport Management*, 2018. doi: 10.4324/9781315630540.

[7] B. F. Santos, M. M. E. C. Wormer, T. A. O. Achola, and R. Curran, “Airline delay management problem with airport capacity constraints and priority decisions,” *Journal of Air Transport Management*, vol. 63, 2017, doi: 10.1016/j.jairtraman.2017.05.003.

[8] Y. Y. Tee and Z. W. Zhong, “Modelling and simulation studies of the runway capacity of Changi Airport,” *Aeronautical Journal*, vol. 122, no. 1253, 2018, doi: 10.1017/aer.2018.48.

[9] L. Thobois, J. P. Cariou, V. Cappellazzo, C. Musson, and V. Treve, “Comparison and validation of wake vortex characteristics collected at different airports by different scanning lidar sensors,” in *EPJ Web of Conferences*, 2018, vol. 176. doi: 10.1051/epjconf/201817606002.

[10] J. Roa, “Technology Development Framework for Air Traffic Control Assisted Airport Procedures in Dynamic Wake Separations,” in *Advances in Intelligent Systems and Computing*, 2019, vol. 786. doi: 10.1007/978-3-319-93885-1_2.

[11] E. Itoh and M. Mitici, “Evaluating the impact of new aircraft separation minima on available airspace capacity and arrival time delay,” *Aeronautical Journal*, vol. 124, no. 1274, 2020, doi: 10.1017/aer.2019.160.

[12] J. N. Hallock and F. Holzäpfel, “A review of recent wake vortex research for increasing airport capacity,” *Progress in Aerospace Sciences*, vol. 98. 2018. doi: 10.1016/j.paerosci.2018.03.003.

[13] V. Cappellazzo, V. Treve, C. Chalon, and I. de Visscher, “Design principles for a separation support tool allowing optimized runway delivery,” 2018. doi: 10.2514/6.2018-4237.

[14] L. Savoni and R. Rudnik, “Pylon Design for a Short Range Transport Aircraft with Over-the-Wing Mounted UHBR Engines.” 2018. doi: 10.2514/6.2018-0011.

[15] A. Keane and P. Keane, “Use of custer channel wings-wing ducts on small UAVs,” *Journal of Aerospace Engineering*, vol. 29, no. 3, pp. 1–10, 2016, doi: 10.1061/(ASCE)AS.1943-5525.0000535.

[16] P. Nishanth, A. Arokkiaswamy, and A. Alen, “Shape optimization of blended-wing-body configuration-an experimental approach,” *International Journal of Recent Technology and Engineering*, vol. 8, no. 1, 2019, doi: 10.2139/ssrn.3507300.

[17] Z. Chen *et al.*, “Assessment on critical technologies for conceptual design of blended-wing-body civil aircraft,” *Chinese Journal of Aeronautics*, vol. 32, no. 8, 2019, doi: 10.1016/j.cja.2019.06.006.

[18] P. Dehpanah and A. Nejat, “The aerodynamic design evaluation of a blended-wing-body configuration,” *Aerospace Science and Technology*, vol. 43, 2015, doi: 10.2514/6.2013-2414.

[19] Willard R Custer, “Aircraft channel wing propeller combination,” 1964

[20] M. A. Md Shafie, M. F. Abdul Hamid, and A. S. Mohd Rafie, “Circulation Control Aircraft Design: Assessment on The Channel-Wing Lift-Thrust Performance Characteristics,” *Journal of Advanced Research in Fluid Mechanics and Thermal Sciences*, vol. 64, no. 1, pp. 143–151, 2019, [Online]. Available: http://www.akademiabaru.com/doc/ARFMTSV64_N1_P143_151.pdf
[21] R. J. Hines, N., Baker, A., Cartagena, M., Largent, M., Tai, J., Qiu, S., Yiakas, N., Zentner, J. and Englar, “Pneumatic Channel Wing Comparative Mission Analysis and Design Study, Phase I,” 2000.
[22] H. Djojodihardjo and N. Thangarajah, “Research, Development and Recent Patents on Aerodynamic Surface Circulation Control - A Critical Review,” *Recent Patents on Mechanical Engineering*, vol. 7, no. 1, pp. 1–37, 2014, doi: 10.2174/2212797607666140204004542.
[23] R. J. Englar, “Development of Pneumatic Channel Wing Powered-Lift Advanced Super-STOL Aircraft,” *20th AIAA Applied Aerodynamics Conference*, no. June, pp. 1–10, 2002, doi: 10.2514/6.2002-2929.
[24] R. Englar and B. Campbell, “Pneumatic Channel Wing Powered-Lift Advanced SuperSTOL Aircraft,” no. June, pp. 1–10, 2012, doi: 10.2514/6.2002-3275.
[25] E. F. Blick and V. Homer, “Power-on channel wing aerodynamics,” *Journal of Aircraft*, vol. 8, no. 4, pp. 234–238, 1970, doi: 10.2514/3.44260.
[26] R. J. Englar and B. A. Campbell, “Development of pneumatic channel wing powered-lift advanced super-STOL aircraft,” *20th AIAA Applied Aerodynamics Conference*, no. June, pp. 1–10, 2002, doi: 10.2514/6.2002-2929.
[27] V. Stanciu and V. Dragan, “An analitical and numerical study of the Custer channel wing configuration,” *International journal of advanced scientific and technical research*, vol. 4, no. 2, pp. 1–8, 2012.

Copyright Statement